Half-Life of ^{138}Xe

Lederer *et al.*[24] list both 17 min and 14 min as half-lives of ^{138}Xe. In order to determine which of the two values was correct we remeasured the independent yield of ^{138}Cs from fission of ^{235}U using our technique and compared that value to the one reported by Wolfsberg.[21] The precision of his measurement was not sensitive to the half-life, since he separated cesium from xenon within a few seconds after fission. Our measurements, however, were extremely sensitive to the half-life of ^{138}Xe since separations were not made until five or more minutes after fission. Using 17 min as the half-life, we calculated a value of 0.12 for the independent yield of ^{138}Cs from fission of ^{235}U, a value in gross disagreement with that of 0.047 reported by Wolfsberg. We found, however, that our calculated yield of ^{138}Cs was consistent with that of Wolfsberg if we used 13.9 min as the half-life of ^{138}Xe. This value is in agreement with previously reported values of 14.0±0.2 min by Clarke and Thode,[26] 14.5±0.5 min by Patzelt and Herrmann,[27] and 14.1±0.8 min by Archer and Keech.[28] We have therefore used 14 min as the half-life of ^{138}Xe.

[26] W. B. Clarke and H. G. Thode, Can. J. Phys. **42**, 213 (1964).
[27] P. Patzelt and G. Herrman, in *Physics and Chemistry of Fission* (International Atomic Energy Agency, Vienna, 1965), Vol. II, p. 243.
[28] N. P. Archer and G. L. Keech, Can. J. Phys. **44**, 1823 (1966).

PHYSICAL REVIEW C VOLUME 1, NUMBER 3 MARCH 1970

Level Structure of Ce^{141} from the $Ce^{140}(n, \gamma)Ce^{141}$ Reaction*

W. Gelletly, J. A. Moragues,† M. A. J. Mariscotti, and W. R. Kane
Brookhaven National Laboratory, Upton, New York 11973
(Received 22 October 1969)

The level scheme of the $_{58}Ce_{83}^{141}$ nucleus was studied by observing the γ rays from the $Ce^{140}(n_{th}, \gamma)$ reaction at the Brookhaven high flux beam reactor. γ-ray singles and coincidence spectra were obtained with a 20-cm^3 Ge(Li) detector and a Ge(Li)-Ge(Li) detector combination. Thirty-two γ rays were assigned to Ce^{141} and all but three of these γ rays were included in the Ce^{141} level scheme. We have identified nine of these transitions as primary transitions from the neutron capture state to low-lying levels in Ce^{141}. These primary transitions have the following energies (in keV) and relative intensities [I(662) = 100]; 4766.6± 0.5(48.0), 4291.4±0.6(22.1), 3619.7±0.6(4.0), 3435.0±0.6(2.0), 3239.0±1.5(2.7), 3092.5±0.5(2.8), 3017.1±0.7(4.7), 3003.3±0.6(3.9), and 2905.9±0.5(3.0). Our data, together with the information available from earlier charged particle reaction and radioactive decay studies, establish levels in Ce^{141} with energies 662.0±0.1, 1137.0±0.3, 1497.3±0.4, 1808.7±0.5, 1994.0±0.6, 2189.6±0.5, 2336.3±1.0, 2410.8± 0.6, 2425.6±0.8, and 2522.9±0.6 keV. The measured neutron separation energy is 5428.6±0.6 keV. All of these levels may be identified with levels observed earlier with lower accuracy in the $Ce^{140}(d, p)Ce^{141}$ reaction. As in the neighboring $N=83$ nuclei Ba^{139} and Nd^{143}, there appears to be a correlation between the strengths of excitation of the $p_{3/2}$ and $p_{1/2}$ levels in the (n, γ) and (d, p) reactions. The 1808.7-keV state, shown here to have $\frac{3}{2}-$ spin and parity and not $\frac{5}{2}-$ as previously believed, exhibits properties typical of a core excitation state formed from the coupling of an $f_{7/2}$ neutron to the first excited $2+$ state of the semimagic Ce^{140} core. In particular, an $E2$ transition proceeds from this state to the $\frac{7}{2}-$ ground state in competition with $M1$ transitions to the $\frac{3}{2}-$ and $\frac{1}{2}-$ first and second excited states. Accordingly, a calculation of the properties of the low-lying excited states in Ce^{141} was carried out on the basis of the weak-coupling model. The results obtained are in reasonable agreement with the measured properties of the levels of Ce^{141}. In particular, it is shown that the measured branching ratios of the transitions from the 1497.3- and 1808.7-keV levels are correctly predicted by this model. The level scheme of Ce^{141} is compared with the level schemes of the other even-Z, $N=83$ nuclei.

I. INTRODUCTION

THE Ce^{141} nucleus has eight protons outside the closed shell at $Z=50$ and one neutron outside the $N=82$ closed shell. The low-lying states of this nucleus are expected to have the relatively simple character associated with the single particle outside the closed shell. Information on the properties of the energy levels of this nucleus is thus of great interest for comparison with the predictions of nuclear models.

Our present limited knowledge of the properties of the energy levels of the Ce^{141} nucleus is derived from studies of the La^{141} β^- decay, the $Ce^{140}(d, p)$ reaction, and the elastic scattering of protons from Ce^{140}.

The decay of 3.8-h La^{141} to levels in Ce^{141} has been studied by Hahn and Strassmann,[1] Katcoff,[2] Duffield and Langer,[3] and Schuman, Turk, and Heath.[4] Their

* Work performed under the auspices of the U.S. Atomic Energy Commission.
† Fellow of the Consejo Nacional de Investigaciones Científicas y Técnicas, Argentina. Present address: Comisión Nacional de Energía Atómica, Buenos Aires, Argentina.
[1] O. Hahn and F. Strassmann, Naturwiss. **27**, 11 (1939); **30**, 324 (1942).
[2] S. Katcoff, in *Radiochemical Studies: The Fission Products* (McGraw-Hill Book Co., New York, 1951), Vol. 9, Paper No. 172.
[3] R. B. Duffield and L. M. Langer, Phys. Rev. **84**, 1065 (1951).
[4] R. P. Schuman, E. H. Turk, and R. L. Heath, Phys. Rev. **115**, 185 (1959).

measurements reveal a very simple decay scheme with ~98% of the La^{141} β^- decays feeding the $\frac{7}{2}-$ ground state[5] of Ce^{141} and the remaining 2% of the decays populating a level at 1370±20 keV. This level, which decays by a single transition to the ground state, has been assigned spin and parity $\frac{9}{2}-$ on the basis of the measured angular momentum of the transferred neutron in the (d, p) reaction[6–8] and the measured logft value[3] for the β transition to this state.

Much more information on the energy levels of the Ce^{141} nucleus has been obtained from the $Ce^{140}(d, p)Ce^{141}$ reaction studies of Holm and Martin,[6] Fulmer, McCarthy, and Cohen,[7] and Wiedner, Heusler, Solf, and Wurm.[8] In addition, Fulmer *et al.*[7] studied the $Ce^{142}(d, t)$ reaction which also leads to levels in Ce^{141}. These groups identified 16 levels in Ce^{141} below 3 MeV. Measurements of the angular distributions of the outgoing protons in the (d, p) reaction allowed them to assign spins to eight of the observed levels. Wiedner *et al.*[8] also measured spectroscopic factors for several of the low-lying levels in the Ce^{141} nucleus.

The isobaric analogs of five of the levels observed in the (d, p) reaction have been studied[9–12] as resonances in the compound nucleus in the elastic scattering of protons from Ce^{140}. Von Brentano, Marquardt, Wurm, and Zaidi,[9] and Zaidi, Von Brentano, Melchior, Rauser, and Wurm[10] reported measurements of the excitation function of the differential cross section for the elastic scattering of protons from Ce^{140}. From these measurements they deduced the spins of the five observed resonances. Veeser, Ellis, and Haeberli[11] measured the polarization of the elastically scattered protons as a function of the incident proton energy. They assigned spins and parities of $\frac{7}{2}-$, $\frac{3}{2}-$, $\frac{1}{2}-$, $\frac{5}{2}-$, and $\frac{5}{2}-$ to the isobaric analog states corresponding to the ground state and excited states at 0.652, 1.136, 1.507, and 1.747 MeV in Ce^{141}. These assignments agree with the results of the (d, p) reaction studies and, with the exception of the second excited state, with the assignments of Von Brentano *et al.*[9] Harney, Wiedner, and Wurm[12] have also reported spectroscopic factors for these levels from studies of the $Ce^{140}(p, p')$ reaction.

Groshev, Dvoretsky, Demidov, and Alvash[13] have studied the $Ce^{140}(n, \gamma)Ce^{141}$ reaction. They report only the energies and intensities of the two most intense primary γ rays. Their results are in good agreement with values of the same quantities reported in an earlier publication[14] by the present authors.

We present here detailed information on the properties of the low-lying energy levels of the Ce^{141} nucleus obtained from a study of the γ rays emitted following the $Ce^{140}(n, \gamma)Ce^{141}$ reaction. The energies and relative intensities of the Ce^{141} γ rays were measured with a 20-cm³ Ge(Li) detector (see Sec. II B). γ-γ coincidences were studied with a Ge(Li)-Ge(Li) detector combination (Sec. II C). A level scheme was then constructed on the basis of all the available data (Sec. III). This level scheme is discussed in Sec. IV. A calculation of the properties of the low-lying levels of Ce^{141} was then carried out on the basis of the weak-coupling model. This calculation is discussed and the results are compared with experiment in Sec. V. In Sec. VI, the level scheme of Ce^{141} is compared with the level schemes of the other even-Z, $N=83$ nuclei.

II. EXPERIMENTAL METHODS AND RESULTS

A. Equipment

The principal target used in these experiments consisted of 12.3 g of CeO_2 enriched in Ce^{140}, with the following isotopic composition[15]: <0.05% Ce^{136}, <0.05% Ce^{138}, 99.61% Ce^{140}, and 0.39% Ce^{142}. In thermal neutron capture, the contributions of the Ce isotopes of masses 136, 138, 140, and 142 to the capture cross section are <0.55, <0.09, 98.72, and 0.64%, respectively. This sample was enclosed in an aluminum capsule. In most of the experimental runs, this target was irradiated in an external, filtered, thermal neutron beam[16] from the Brookhaven high flux beam reactor with an intensity of $\sim 7\times10^7$ neutrons/sec over 1 cm² and a Cd ratio of $\approx 2\times10^4$. In a few runs, the same target was irradiated in an external, diffracted neutron beam[16] with an energy of 0.08 eV and an intensity of $\sim 10^5$ neutrons/sec over 1 sq. in.

Targets of natural CeO_2 and natural $Ce(NO_3)_3$ were used to study the γ-ray spectrum from thermal neutron capture on natural cerium. A piece of graphite was also used as a target in order to obtain a measure of the background radiation.

---

[5] R. W. Kedzie, M. Abraham, and C. D. Jeffries, Phys. Rev. **108,** 54 (1957).
[6] G. B. Holm and H. J. Martin, Jr., Phys. Rev. **122,** 1537 (1961).
[7] R. H. Fulmer, A. L. McCarthy, and B. L. Cohen, Phys. Rev. **128,** 1302 (1962).
[8] C. A. Wiedner, A. Heusler, J. Solf, and J. P. Wurm, Nucl. Phys. **A103,** 433 (1967).
[9] P. Von Brentano, N. Marquardt, J. P. Wurm, and S. A. A. Zaidi, Phys. Letters **17,** 124 (1965).
[10] S. A. A. Zaidi, P. Von Brentano, K. Melchior, P. Rauser, and J. P. Wurm, in *Isobaric Spin in Nuclear Physics,* edited by J. D. Fox and D. Robson (Academic Press Inc., New York, 1966), p. 798.
[11] L. Veeser, J. Ellis, and W. Haeberli, Phys. Rev. Letters **18,** 1063 (1967).
[12] M. L. Harney, C. A. Wiedner, and J. P. Wurm, Phys. Letters **26B,** 204 (1968).
[13] L. V. Groshev, V. N. Dvoretsky, A. M. Demidov, and M. S. Alvash, Kurchatov Atomic Energy Institute Report No. IAE-1780, 1969 (unpublished).
[14] M. A. J. Mariscotti, J. A. Moragues, W. Gelletly, and W. R. Kane, Phys. Rev. Letters **22,** 303 (1968).
[15] The target material was obtained from the Stable Isotopes Division, Oak Ridge, Tenn.
[16] W. R. Kane, D. Gardner, T. Brown, A. Kevey, E. der Mateosian, G. T. Emery, W. Gelletly, M. A. J. Mariscotti, and I. Schroder, Bull. Am. Phys. Soc. **14,** 514 (1969).

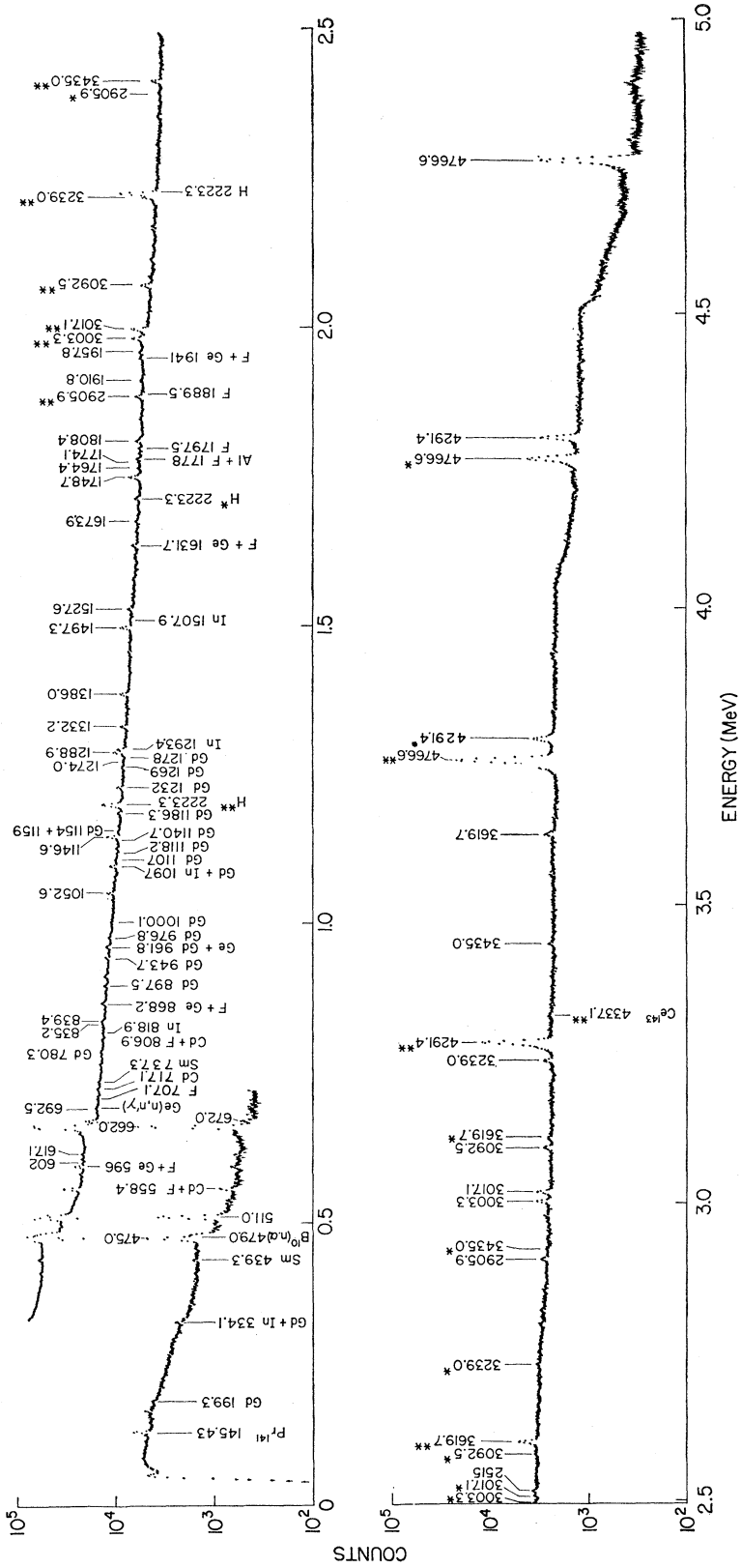

FIG. 1. An example of the γ-ray spectrum from the Ce target enriched in Ce^{140} over the energy range 100 keV–5.0 MeV plotted on a semilogarithmic scale. The target was irradiated in an external, filtered, thermal neutron beam (Ref. 16) at the Brookhaven high flux beam reactor. The spectrum was accumulated in a run of $16\frac{1}{4}$ h duration. Below ~660 keV, the spectrum exceeded the analyzer memory capacity several times. A short run of ~45 min duration has also been plotted in order to show the low-energy portion of the spectrum. Those lines belonging to Ce^{141} are indicated on the figure. Single and double asterisks indicate one- and two-escape peaks, respectively. The origins of some of the many background lines are also indicated on the figure. The three peaks due to the intense 4766.6- and 4291.4-keV primary γ rays to the first and second excited states of Ce^{141} are clearly seen in the lower part of the figure. The weak two-escape peak of the 4337.1-keV transition in Ce^{143} is just visible in this spectrum. This spectrum should be compared with the γ-ray spectrum from natural CeO_2 which is shown in Fig. 2.

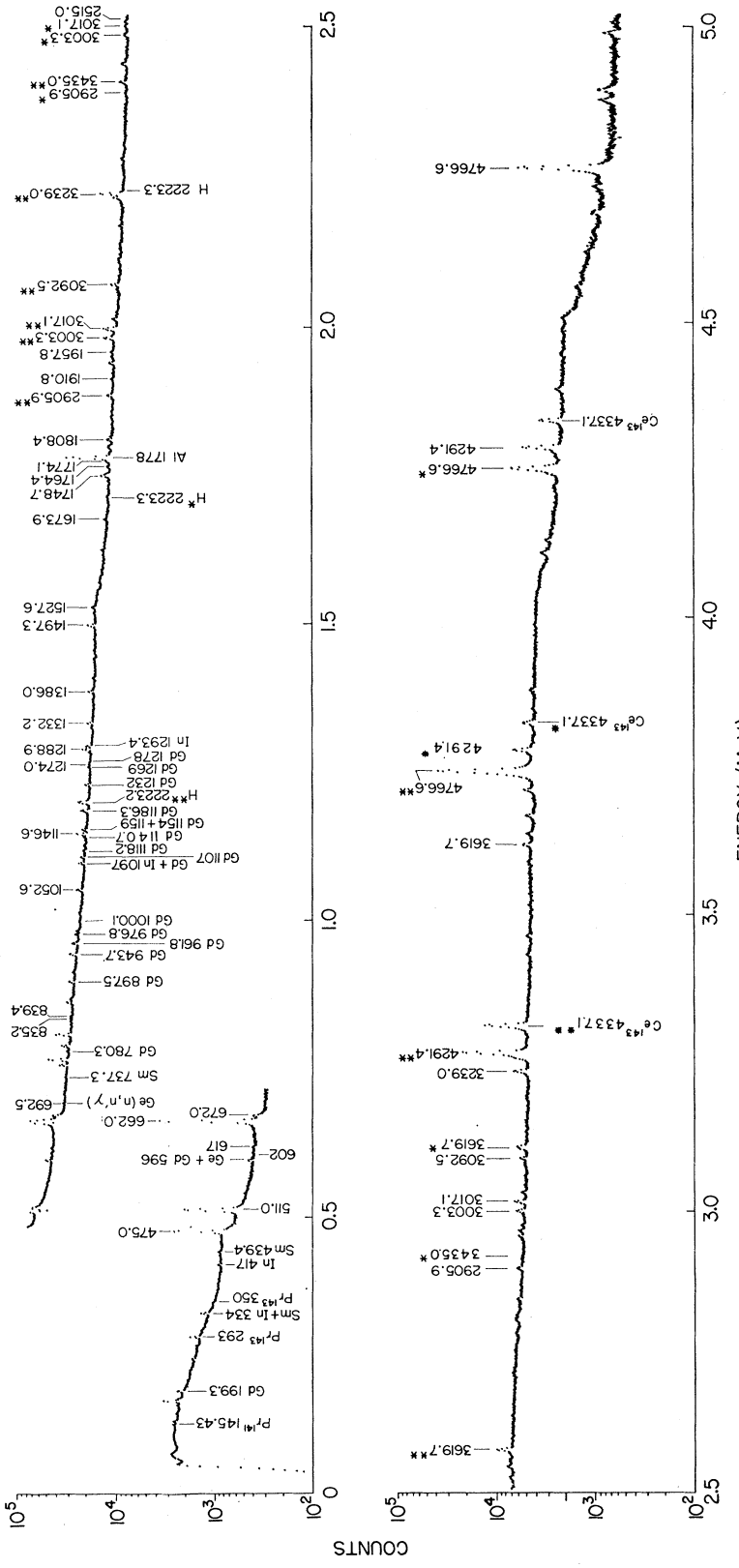

FIG. 2. An example of the γ-ray spectrum from natural CeO_2 over the energy range 100 keV–5.0 MeV plotted on a semilogarithmic scale. The target was irradiated in an external, filtered, thermal neutron beam (Ref. 16) at the Brookhaven high flux beam reactor. The spectrum was accumulated in a run of $16\frac{1}{4}$ h duration. Below 660 keV, the spectrum exceeded the analyzer memory capacity several times. A short run of $\sim 1\frac{1}{2}$ h duration has also been plotted up to 700 keV in order to show the low-energy region of the spectrum. Single and double asterisks indicate one- and two-escape peaks, respectively. Those lines assigned to Ce^{141} are indicated on the figure. The origins of some of the background lines are also indicated on the figure. The peaks due to the intense 4766.6- and 4291.4-keV primary γ rays in Ce^{141} and the intense 4337.1-keV primary γ ray in Ce^{143} are clearly visible in the lower half of the figure. This spectrum should be compared with the γ-ray spectrum from the sample enriched in Ce^{140}, which is shown in Fig. 1.

TABLE I. Energies, relative intensities, and assignments of γ rays observed in the $Ce^{140}(n, \gamma)Ce^{141}$ reaction.

E_γ (keV)	I_γ (relative)	Level (keV) from	Level (keV) to	$\Delta L - E_\gamma$ [a] (keV)
475.0±0.2[b]	29±12	1137.0	−662.0	...
602±1	0.3±0.3	2410.8	−1808.7	0.1±1.3
617.1±0.6	0.4±0.2	2425.6	−1808.7	−0.2±1.1
662.0±0.1[b]	100±6	662.0	−g.s.	...
672.0±0.8	1.4±0.4	1808.7	−1137.0	−0.3±1.0
692.5±0.4	...	2189.6	−1497.3	−0.2±0.7
835.2±1.0	0.4±0.3	1497.3	−662.0	0.1±1.1
839.4±0.6	0.6±0.3	2336.3	−1497.3	−0.4±1.1
1052.6±0.4	1.8±0.4	2189.6	−1137.0	0±0.9
1146.6±0.3	2.9±0.5	1808.7	−662.0	0.1±0.6
1274.0±1.5	0.3±0.2	2410.8	−1137.0	−0.2±1.6
1288.9±1.0	2.4±0.6	2425.6	−1137.0	−0.3±1.4
1332.2±0.4	1.9±0.4	1994.0	−662.0	−0.2±0.7
1386.0±0.4	1.9±0.4	2522.9	−1137.0	−0.1±0.8
1497.3±0.4	2.8±0.8	1497.3	−g.s.	...
1527.6±0.6	1.4±0.3	2189.6	−662.0	0±0.8
1673.9±1.0	0.5±0.2	2336.3	−662.0	0.4±1.4
1748.7±0.5	3.4±0.5	2410.8	−662.0	0.1±0.8
1764.4±1.0	0.7±0.3	2425.6	−662.0	−0.8±1.4
1774.1±1.0[c]	0.7±0.4			
1808.4±0.7	1.7±0.5	1808.7	−g.s.	0.3±0.9
1910.8±0.7	0.8±0.2			
1957.8±0.8	1.0±0.5			
2515±1	0.6±0.3			
2905.9±0.5	3.0±0.7	5428.6	−2522.9	−0.2±1.0
3003.3±0.6	3.9±0.6	5428.6	−2425.6	−0.3±1.2
3017.1±0.7	4.7±0.6	5428.6	−2410.8	0.7±1.1
3092.5±0.5	2.8±0.6	5428.6	−2336.3	−0.2±1.1
3239.0±1.5	2.7±0.6	5428.6	−2189.6	0±1.6
3435.0±0.6	2.0±0.4	5428.6	−1994.0	−0.4±1.0
3619.7±0.6	4.0±0.9	5428.6	−1808.7	0.2±1.0
4291.4±0.6[b]	22.1±2.4	5428.6	−1137.0	0.1±0.9
4766.6±0.5[b]	48.0±4.8	5428.6	−662.0	−0.1±0.8

[a] ΔL denotes the difference in energy of the levels between which the transition takes place minus the recoil energy. Three dots in this column indicate that the γ-ray energy was used to determine the level energy. No entry in this column indicates that the γ ray could not be placed in the level scheme.

[b] The measured energies of these γ rays were used to determine the neutron separation energy.

[c] This γ ray belongs to Ce, but it was not possible to assign it to a particular isotope because of the presence in the natural Ce spectrum of an intense γ ray of 1778 keV from the aluminum capsule.

The singles γ-ray spectra were measured with an $\sim$20-cm^3 Ge(Li) detector. Coincidences between γ rays were studied with this detector and a 9-cm^3 Ge(Li) diode in 90° geometry.

The electronic equipment used in these experiments and the procedure for analysing the data have been described in an earlier publication.[17]

B. Energy and Intensity Measurements

The γ-ray singles spectrum from the $Ce^{140}(n, \gamma)Ce^{141}$ reaction was measured over the energy range 100 keV–5 MeV in several runs of different dispersion and energy range. Figure 1 shows an example of the γ-ray spectrum from the enriched Ce^{140} target from 100 keV–5 MeV. This spectrum was accumulated in a run of $\approx$16 h duration with the external, filtered, thermal neutron beam collimated to a diameter of 3.0 mm. Below 660 keV, this spectrum had exceeded the analyser memory capacity several times. A short run of $\approx$45 min duration, which was taken under the same experimental conditions, has also been plotted in Fig. 1 in order to show this low-energy portion of the spectrum. Single and double asterisks have been used to indicate one- and two-escape peaks.

Because of the small thermal neutron capture cross section of Ce^{140} many lines from the background and from other target materials are of comparable intensity to the Ce^{141} γ-ray lines. In order to distinguish the Ce^{141} γ-ray lines from the background lines, the γ-ray spectrum from the enriched Ce^{140} target was carefully

[17] M. A. J. Mariscotti, W. Gelletly, J. A. Moragues, and W. R. Kane, Phys. Rev. **174,** 1485 (1968).

compared with the γ-ray spectra from the natural CeO_2 target and the background. An example of the γ-ray spectrum fron the natural CeO_2 target over the energy range 100 keV–5 MeV is shown in Fig. 2. Those γ rays assigned to the $Ce^{140}(n, \gamma)Ce^{141}$ reaction are listed in Table I.

The energies of the Ce^{141} γ rays were measured from spectra taken with a natural $Ce(NO_3)_3$ target and a mixed Cr^{53} and CeO_2 target. At intervals during the measurement of these spectra, the spectrum was routed into a separate section of the analyser memory and a set of pulser peaks from a precision pulser was superimposed on the γ-ray spectrum. This allowed us to compare the energies of the Ce^{141} γ rays with the energies of the neutron capture γ rays from the $N^{14}(n, \gamma)N^{15}$ and $Cr^{53}(n, \gamma)Cr^{54}$ reactions. The energies of the N^{15} γ rays have been precisely determined by Greenwood,[18] and the energies of the Cr^{54} γ rays have been measured by Kane, Mariscotti, and Emery,[19] and by White, Groves, and Birkett.[20] The energy separations between the Ce γ-ray peaks and the Cr^{54} and N^{15} calibration lines were first determined in units of pulse height from the pulser. The pulse-height differences were then converted into energy units by using the known energy differences between the calibration peaks. This procedure assumes that there is a linear relationship between the pulse heights from the γ-ray detector and the pulser, and between pulse height and the channel number of the observed peak over the short, intervening regions between the peaks. The measured energies E_γ of the γ rays assigned to Ce^{141} are shown in column 1 of Table I.

Column 3 of Table I shows the initial and final levels between which the γ-ray transition occurs. Column 4 gives $\Delta L - E_\gamma$, where ΔL is the difference in energy of the levels between which the transition takes place minus the recoil energy. Three dots in this column indicate that the γ-ray energy was used to determine the level energy. No entry in columns 3 and 4 indicates that the γ ray could not be placed in the level scheme.

The relative intensities of the Ce^{141} γ rays were measured and are given in column 2 of Table I. These intensities were obtained with the use of a relative efficiency curve for the 20-cm³ Ge(Li) detector which was obtained in the manner described by Kane and Mariscotti.[21]

C. γ-γ Coincidence Measurements

The 20-cm³ Ge(Li) detector was also used in combination with a 9-cm³ Ge(Li) detector to measure γ-γ coincidences. Pulses from both detectors were stored in the TMC analyzer in a 128×128-channel format. Two separate runs were made. In the first run, the γ rays from 250 to 890 keV detected in the 9-cm³ Ge(Li) detector were studied in coincidence with the γ rays from 980 to 1480 keV detected in the 20-cm³ Ge(Li) detector. In the second run, the γ rays from 300 to 1500 keV detected in the 9-cm³ detector were studied in coincidence with the γ rays from 2300 to 3900 keV detected in the 20-cm³ detector. Because of the small thermal neutron capture cross section of

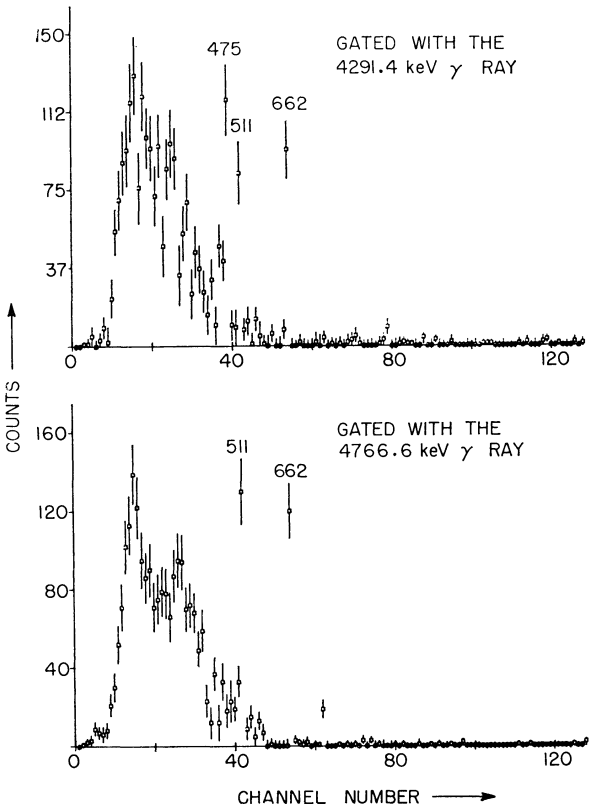

FIG. 3. This figure shows the net coincidence spectra from the 9-cm³ Ge(Li) detector gated with the two escape peaks of the 4291.4- and 4766.6-keV γ rays which were detected in the 20-cm³ Ge(Li) detector. These spectra cover the energy range 300–1500 keV. Each spectrum was obtained as a computer output from the program PALMUD (Ref. 22), which sums the spectrum slices associated with the gating γ ray and subtracts an equal number of background slices. It should be noted that this procedure does not include the subtraction of chance coincidences from the spectrum. Chance coincidences are not a significant fraction of the total counts in these spectra. At the energy dispersion used (9.4 keV/channel), a γ-ray photo-peak appears in a single channel. The figure shows clearly that the 4291.4-keV transition is in coincidence with both the 475.0- and 662.0-keV γ rays while the 4766.6-keV transition is in coincidence with the 662.01-keV γ ray alone. This result confirms the assignment of the 4766.6- and 4291.4-keV transitions as primary transitions from the capture state to the first and second excited states at 662.01 and 1137.01 keV, respectively (see text).

[18] R. C. Greenwood, Phys. Letters **27B**, 274 (1968).
[19] W. R. Kane, M. A. J. Mariscotti, and G. T. Emery (private communication).
[20] D. H. White, D. J. Groves, and R. E. Birkett, Nucl. Instr. Methods **66**, 70 (1968).
[21] W. R. Kane and M. A. J. Mariscotti, Nucl. Instr. Methods **56**, 189 (1967).
[22] M. A. J. Mariscotti, Nucl. Instr. Methods **50**, 309 (1967); Brookhaven Laboratory Report No. BNL 10904 (unpublished).

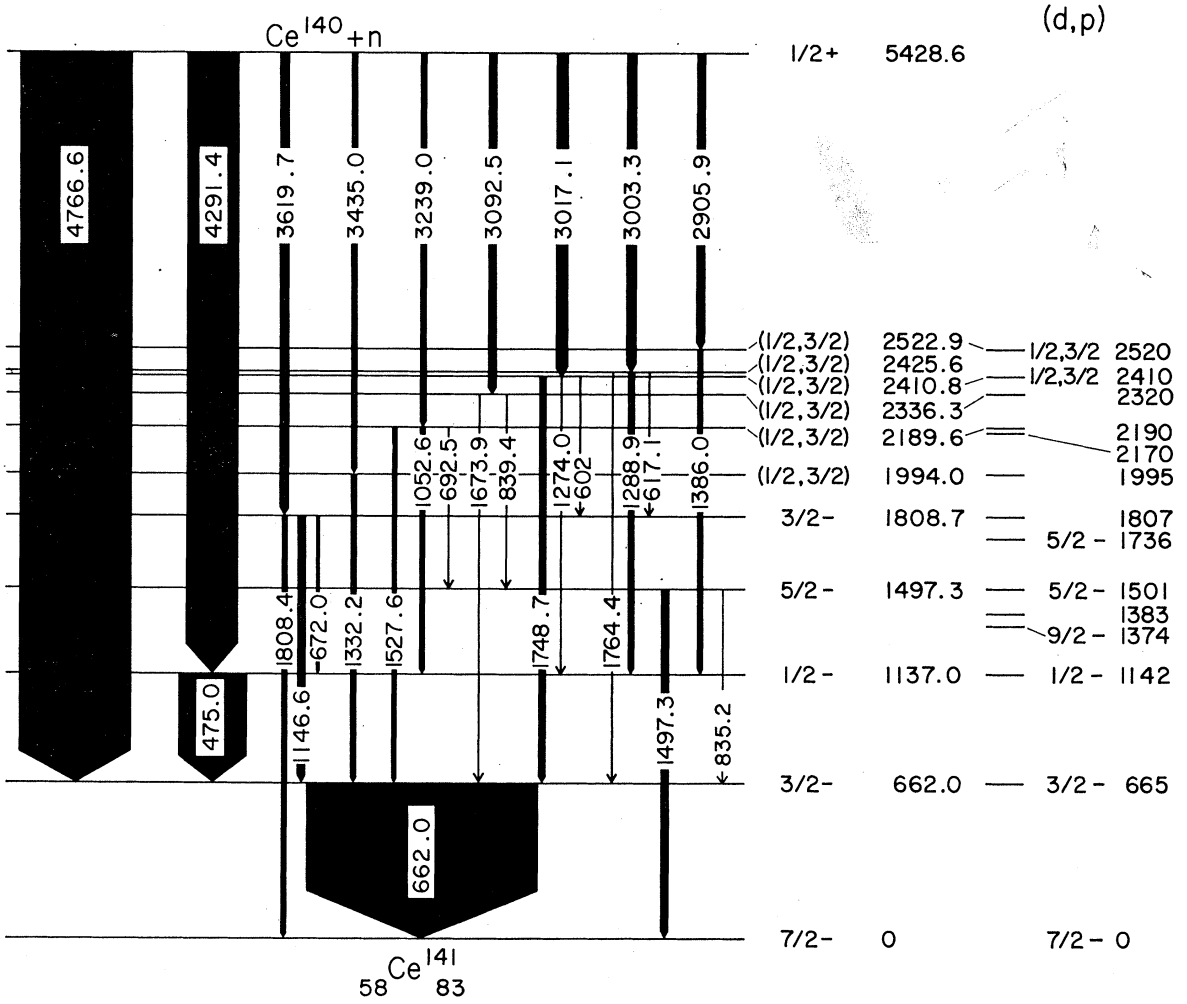

FIG. 4. The level scheme of Ce^{141} obtained from the study of the $Ce^{140}(n, \gamma)Ce^{141}$ reaction. The measured level energies in keV and assigned spins and parities are indicated on the right. The level energies and spin assignments from the $Ce^{140}(d, p)Ce^{141}$ reaction studies (Refs. 6–8) are shown on the extreme right. Below the level at 2190 keV the energies quoted on the extreme right are taken from the work of Wiedner *et al.* (Ref. 8). The remaining energy values are those of Fulmer *et al.* (Ref. 7). It should be noted that the level energies measured by Wiedner *et al.* (Ref. 8) agree with those obtained in the present work within the experimental error. The breadths of the vertical lines are proportional to the measured relative intensities of the transitions they represent. The measured transition energies in keV are marked on the figure. The level observed at 1374 keV in the (d, p) reaction studies (Refs. 6–8) may be identified with the level observed (Refs. 3, 4) at 1370±20 keV in the decay of La^{141} (see text). This level decays to the ground state by a 1370± 20-keV transition.

Ce^{140} the counting rates in these experiments were low. As a result great care had to be exercised in interpreting these spectra since coincidences due to γ rays from the target contaminants and from the background were also observed.

Only the strongest γ ray cascades are clearly seen in the coincidence spectra. The two best examples, from the second run, of the spectrum in the 9-cm^3 detector in coincidence with a single peak detected in the 20-cm^3 detector are shown in Fig. 3. The upper spectrum shows the spectrum in coincidence with the two-escape peak of the 4291.4-keV primary γ ray. Both the 475- and 662-keV γ rays are clearly present. The lower spectrum shows the spectrum gated with the two-escape peak of the 4766.6-keV primary γ ray. In this case, only the 662-keV γ ray is present. It should be noted that random coincidences have not been subtracted from these spectra. They do not contribute a significant fraction of the total counts in these spectra.

The results of the coincidence measurements are summarized in Table II.

III. CONSTRUCTION OF THE LEVEL SCHEME

The level scheme of Ce^{141}, which is shown in Fig. 4, was constructed from the data of Table I, the γ-γ

coincidence measurements, and the information available from previous studies of this nucleus.

A firm basis for the construction of the level scheme is provided by the assumption that the intense transitions of energies 4766.6 and 4291.4 keV (see Figs. 1 and 2) are primary transitions from the neutron capture state to the first and second excited states of Ce^{141}. This assumption is supported by the following observations:

(a) The (d, p) and (p, p') reaction studies[6–11] indicate levels in Ce^{141} at 665 and 1142 keV of spin and parity $\frac{3}{2}-$ and $\frac{1}{2}-$, respectively. Thermal neutron capture on Ce^{140} (ground-state spin and parity $0+$) leads to a capture state of spin and parity $\frac{1}{2}+$. Hence one may expect to observe $E1$ primary transitions from the capture state to these levels but not an $E3$ primary transition to the $\frac{7}{2}-$ ground state of Ce^{141}.

(b) In the low-energy region of the Ce^{141} γ-ray spectrum, we observe two intense γ rays of energies 662.0 and 475.0 keV (see Figs. 1 and 2). The former energy and the sum of these two energies [662.0+475.0=1137.0 keV] are in good agreement with the energies of the first two levels observed in the (d, p) reaction [see (a) above]. The energy 475.0 keV also agrees well with the difference in energy (475.2 keV) between the 4766.6- and 4291.4-keV γ rays.

(c) The coincidence results clearly support this interpretation. As Fig. 3 shows, the 4766.6-keV transition is in coincidence with the 662-keV γ ray alone, while the 4291.4-keV transition is in coincidence with both the 662- and 475-keV transitions.

These observations establish the first and second excited states at 662.0 and 1137.0 keV. The remainder of the level scheme was then constructed as follows: (1) First the neutron separation energy was determined from the 4766.6-662.0 and 4291.4-475.0-662.0 keV γ-ray cascades. The weighted average value of the neutron separation energy, corrected for the nuclear recoil energy, was found to be 5428.6±0.6 keV, in agreement with the value of 5438±9 keV given by Mattauch, Thiele, and Wapstra.[23] (2) It was then assumed that each of the observed γ rays was a primary γ ray. The difference in energy between the measured neutron separation energy and the γ-ray energy gave a preliminary value for the level energy (E_L). (3) A search of the γ-ray singles spectrum was then made for the presence of secondary γ rays whose energies equalled the difference in energy between E_L and the energies of levels of lower energy which had already been established. In general, the secondary γ rays were placed in the level scheme on the basis of the energy fit, but in some cases the placing of the transition was supported by the coincidence results. At least one incoming and one outgoing transition were observed in the case of each of the levels finally established. Each of these levels was also observed in the (d, p) reaction. (4) A precise value for E_L was then determined from the weighted mean of values obtained from all transitions into and out of the level. (5) Steps 3 and 4 were then repeated using the readjusted values of E_L.

[23] J. H. E. Mattauch, W. Thiele, and A. H. Wapstra, Nucl. Phys. **67**, 32 (1965).

TABLE II. Results of the γ-γ coincidence measurements.

(A) High-energy–low-energy coincidences[a]

γ ray (keV)	Coincident peaks (keV)[b]
475.0	4291.4**, 3619.7**
662.0	4766.6**, 4291.4**, (3619.7**)
3619.7**	475.0, 662.0
4291.4**	475.0, 662.0
4766.6**	662.0

(B) Low-energy–low-energy coincidences

475.0	1052.6, 1288.9, 1386.0
662.0	(1052.6), 1146.6, 1288.9
1052.6	475.0, (662.0)
1288.9	475.0, 662.0
1386.0	475.0, 662.0

[a] The double asterisk indicates that the two-escape peak of the γ ray was observed.

[b] Brackets indicate that the observed coincidence peak is weak.

Comments on the properties of the individual levels in Ce^{141} follow.

A. Levels at 662.0±0.1 and 1137.0±0.3 keV

These levels, the first and second excited states in Ce^{141}, were established in the manner described above. They are strongly excited in the $Ce^{140}(d, p)$ and $Ce^{142}(d, t)$ reactions and their isobaric analogs were observed in the $Ce^{140}(p, p')$ reaction studies.[9–11] The observation of the intense 4766.6- and 4291.4-keV primary transitions to these levels is consistent with the $\frac{3}{2}-$ and $\frac{1}{2}-$ spin and parity assignments of Veeser *et al.*[11]

As one would expect from the $\frac{1}{2}-$ spin and parity assignment to the 1137-keV level, no cross-over γ ray of 1137 keV to the $\frac{7}{2}$ ground state was observed.

B. Level at 1497.3±0.4 keV

A level at 1501 keV with $l_n=3$ was observed in the (d, p) reaction studies.[7,8] It was assigned spin $\frac{5}{2}$ in agreement with the $\frac{5}{2}-$ spin and parity assignment from the isobaric analog resonance studies of Von Brentano *et al.*[9] and Veeser *et al.*[11]

This level is fed by the weak 692.5- and 839.4-keV transitions from the 2189.6- and 2336.3-keV levels. It is not fed from the $\frac{1}{2}+$ neutron capture state. It decays to the ground state and first excited state

by the 1497.3- and the weak 835.2-keV transitions. These observations are consistent with the $\frac{5}{2}-$ spin and parity assignment.

It should be noted that the total intensity of the outgoing transitions from this level greatly exceeds the total intensity of the transitions to the level.

C. Level at 1808.7±0.5 keV

This level is fed from the capture state by the 3619.7-keV transition. It is also fed by the weak 602- and 617.1-keV transitions from the levels at 2410.8 and 2425.6 keV. It decays by the 1808.4-, 1146.6-, and 672.0-keV transitions to the ground state, 662.0-keV state, and 1137.0-keV states, respectively. Both the 3619.7- and 1146.6-keV γ rays were observed to be in coincidence with the 662-keV γ rays deexciting the first excited state.

This level may be identified with the 1807-keV level observed in the (d, p) reaction studies.[6,8] It was tentatively assigned $l_n=3$ by Fulmer *et al.*[7] indicating spin $\frac{5}{2}$ or $\frac{7}{2}$. The observed feeding from the $\frac{1}{2}+$ capture state and the decay to levels of spins and parities $\frac{1}{2}-$, $\frac{3}{2}-$, and $\frac{7}{2}-$ indicates that spin and parity $\frac{3}{2}-$ is the most probable assignment.

D. Level at 1994.0±0.6 keV

This level is fed from the capture state by the 3435.0 keV transition and decays by the 1332.2-keV transition to the 662.0-keV first excited state.

It was not possible to rule out the presence of a 185.3-keV transition to the 1808.7-keV level because of the presence of an intense background line at this energy.

Fulmer *et al.*[7] tentatively assigned $l_n=1$ to this level in their (d, p) reaction studies which indicates spin $\frac{1}{2}$ or $\frac{3}{2}$. This assignment is consistent with our results.

E. Level at 2189.6±0.5 keV

This level is populated by the 3239.0-keV primary transition and decays to the 662.0-, 1137.0-, and 1497.3-keV levels by the 1527.6-, 1052.6-, and 692.5-keV transitions. The 692.5-keV γ ray is very weak and is masked by the broad 690-keV peak produced by scattered neutrons in the Ge detector following the $\mathrm{Ge}(n, n')$ reaction. A careful comparison of the Ce and background γ-ray spectra in this energy region indicates that a weak transition of this energy belongs to Ce^{141} although it was not possible to measure its intensity.

Wiedner *et al.*[8] reported levels in Ce^{141} at 2170 and 2190 keV from their (d, p) reaction studies. Fulmer *et al.*,[7] with an experimental resolution of 60 keV, observed a single level at 2180 keV with $l_n=3$. In the (n, γ) reaction a primary transition was observed to the level at 2189.6 keV. No primary transition to a level at 2170 keV was observed. We conclude that (i) the level at 2189.6 keV has spin $\frac{1}{2}$ or $\frac{3}{2}$ and may be identified with the level observed at 2190 keV by Wiedner *et al.*; (ii) the level at 2170 keV has spin $\frac{5}{2}$ or $\frac{7}{2}$. The latter conclusion would account for the failure to observe a primary transition to the level in the (n, γ) reaction and the assignment of $l_n=3$ to the unresolved 2180-keV doublet by Fulmer *et al.*[7]

F. Level at 2336.3±1.0 keV

This level is fed by the 3092.5-keV transition from the capture state, and decays to the 662.0- and 1497.3-keV levels by the weak 1673.9- and 839.4-keV transitions.

This level may be identified with the level at 2320 keV observed by Fulmer *et al.*[7] in the $\mathrm{Ce}^{140}(d, p)$ reaction. The difference in energy lies within the error of their measurements and is consistent with the observed differences of $+8$ to -20 keV between their measurements of other level energies and those obtained in the present work.

The possible transition to the 1137.0-keV second excited state has the energy 1199.2 keV. A γ ray of this energy is masked by the two-escape peak of the hydrogen capture γ ray. From our knowledge of the relative intensities of the two-escape and full-energy peaks for the 2223.3-keV hydrogen line in our 20-cm^3 Ge(Li) detector we conclude that the intensity of the possible 1199.2-keV line is less than 1% of that of the 662-keV γ ray (i.e., less than twice the intensity of the 1673.9-keV γ ray). It was not possible to determine whether a 146.6-keV transition to the level at 2189.6 keV exists because of the presence in this spectrum of the intense 145.3-keV γ ray in Pr^{141} following the decay of Ce^{141}.

It should be noted that the intensity of the incoming 3092.5-keV transition is more than twice the total intensity of the observed outgoing transitions.

A spin of $\frac{1}{2}$ or $\frac{3}{2}$ is suggested by the observation of the primary transition from the $\frac{1}{2}+$ capture state.

G. Level at 2410.8±0.6 keV

This level is fed by the 3017.1-keV primary transition. It decays to the 662.0-, 1137.0-, and 1808.7-keV levels by the 1748.7-, 1274.0-, and 602-keV transitions.

A level at this energy with $l_n=1$ was observed in the (d, p) reaction by Fulmer *et al.*[7] and by Holm and Martin.[6] This level would not be resolved from the level at 2425.6 keV in their experiments.

A spin of $\frac{1}{2}$ or $\frac{3}{2}$ is suggested by the present results.

H. Level at 2425.6±0.8 keV

This level is fed from the capture state by the 3003.3-keV transition and decays to the 662.0-, 1137.0-, and 1808.1-keV levels by the 1764.4-, 1288.9-, and 617.1-keV transitions. These results suggest a spin of $\frac{1}{2}$ or $\frac{3}{2}$.

I. Level at 2522.9±0.6 keV

This level is populated by the 2905.9-keV transition from the capture state and decays to the second excited state at 1137.0- by the 1386.0-keV transition.

A possible 333.3-keV transition to the 2189.6-keV level is obscured by the In and Gd lines of the same energy. A transition of 186.6-keV energy, which would fit in energy between this level and the 2336.3-keV level, was observed in the spectrum from both the enriched and natural targets, but its intensity is enhanced in the spectrum from the natural sample. Some portion of this line may belong to Ce^{141}.

This level may be identified with the level at 2520 keV observed in the (d, p) reaction by Fulmer *et al.*[7] This level was assigned $l_n=1$ by these authors indicating a spin of $\frac{1}{2}$ or $\frac{3}{2}$ in agreement with the present results.

IV. DISCUSSION

The final level scheme for Ce^{141}, which is shown in Fig. 4, includes all but three of the transitions assigned to Ce^{141} in the present work (see Table I). One test of the completeness of the level scheme is the balance of intensity within it. With the two exceptions noted in Sec. III there is a balance in intensity between the incoming and outgoing transitions for the levels in Ce^{141} observed in the present work. The total intensity of transitions feeding the 662.0-keV first excited state is 98.2% of the intensity of the 662.0-keV transition deexciting the level to the ground state. In addition, the total intensity of the primary capture γ rays deexciting the neutron capture state is 89% of the total intensity of the transitions to the Ce^{141} ground state.

All of the levels observed in the (n, γ) reaction correspond in energy to levels observed in the $Ce^{140}(d, p)Ce^{141}$ reaction studies[6–8] within the errors of the latter work. Those levels below 2 MeV which are excited in the two reactions are almost certainly identical. At higher energies it is evident from the errors in the (d, p) studies and the level density that the levels excited are probably, but not necessarily identical. Where a level has been observed in both the (n, γ) and (d, p) reactions, the (n, γ) results are consistent with the measured values of the angular momentum of the transferred neutron in the (d, p) reaction, with the exception of the level at 1808.7 keV (see Sec. III C).

As mentioned earlier, the isobaric analogs of the first four excited states in Ce^{141} have been studied by Von Brentano *et al.*,[9] Zaidi *et al.*,[10] Veeser *et al.*,[11] and by Harney *et al.*[12] The observation of primary neutron capture γ rays from the $\frac{1}{2}+$ capture state to the levels at 662.0, 1137.0, and 1808.7 keV and the failure to observe a transition to the level at 1497.3 keV are consistent with the spins and parities assigned by Veeser *et al.*[11]

The level observed at 1374 keV in the (d, p) reaction studies[6–8] and assigned $l_n=5$ may be identified with the level at 1370±20 keV observed[3,4] in the decay of La^{141}. The $\frac{9}{2}-$ assignment to this level is clearly consistent with our failure to observe this level following the $Ce^{140}(n, \gamma)$ reaction which preferentially populates levels of spin $\frac{1}{2}$ or $\frac{3}{2}$.

The most striking feature of the level scheme is the intense feeding of the first and second excited states from the neutron capture state. These levels are also strongly excited in the (d, p) reaction and have spectroscopic factors of 0.42 and 0.38, respectively. As in the case of the other $N=83$ nuclei, Ba^{139} and Nd^{143}, a strong correlation exists between the strengths of excitation of these levels in the (n, γ) and (d, p) reactions.[14] This behavior has been shown[14,24] to be consistent with the common unique parent assumption of Lane and Wilkinson[25] and with the predominance of direct capture in the $Ce^{140}(n, \gamma)Ce^{141}$ reaction. A comparison of the (n, γ) and (d, p) strengths for the higher excited states of Ce^{141} with $l_n=1$ must await the measurement of their respective spectroscopic factors.

V. WEAK-COUPLING DESCRIPTION OF LOW-LYING STATES IN Ce^{141}

A. Properties of Levels in Ce^{141}

Since Ce^{141} has one neutron outside the closed neutron shell at $N=82$, we expect the low-lying excited states of this nucleus to exhibit a predominantly single-particle character. The spin and parity $\frac{7}{2}-$ as well as the large spectroscopic factor[8,12] of the ground state indicate that, indeed, this state may be attributed largely to an $f_{7/2}$ neutron coupled to the 0+ ground state of the Ce^{140} core. Similarly, on the basis of their measured spectroscopic factors, the $\frac{3}{2}-$ state at 662.01 keV, the $\frac{1}{2}-$ state at 1137.0 keV, the $\frac{9}{2}-$ state at 1374 keV [not observed in the (n, γ) reaction], and the $\frac{5}{2}-$ state at 1497.3 keV contain a large fraction of the single-particle strength of the $p_{3/2}$, $p_{1/2}$, $h_{9/2}$, and $f_{5/2}$ orbits, respectively. With the exception of the $i_{13/2}$ orbit these are all of the expected shell-model orbits between the $N=82$ and $N=126$ closed shells.

Besides the five states mentioned above, two more states of Ce^{141} are of known spin and parity; namely, the $\frac{5}{2}-$ state at 1736 keV [only observed in the (d, p) reaction] and the $\frac{3}{2}-$ state at 1808.7 keV. (Hereinafter we shall refer to these states as the $\frac{5}{2}-'$ and $\frac{3}{2}-'$ states.) The properties of the 1808.7-keV $\frac{3}{2}-'$ state are of particular interest. The three transitions which depopulate this state have comparable intensities, although the ground-state transition has $E2$ multipolarity while those to the first and second ex-

[24] J. A. Moragues, M. A. J. Mariscotti, W. Gelletly, and W. R. Kane, Phys. Rev. **180**, 1105 (1969).
[25] A. M. Lane and D. H. Wilkinson, Phys. Rev. **97**, 1199 (1955).

TABLE III. Parameters used in the calculation of the properties of excited states in Ce^{141}.

Parameter	Value	Reference
Phonon energy	$\hbar\omega=1.596$ MeV	First excited 2+ state of Ce^{140}
Restoring force constant	$C=366$ MeV or $\hbar\omega/2C=2\times10^{-3}$	Deduced from measured $B(E2, 0^+\rightarrow2^+)$ for Ce^{140} (30 and 31)
Radial matrix element	$k=40$ MeV	26
Core g factor	$g_R=0.95$	32
Single-particle energies (relative to $\epsilon_{f7/2}=0$)	$\epsilon_{p3/2}=1.2$ MeV $\epsilon_{p1/2}=1.5$ MeV $\epsilon_{f5/2}=1.7$ MeV	Arranged to fit the energies of first $\frac{3}{2}-$, $\frac{1}{2}-$, and $\frac{5}{2}-$ excited states in Ce^{141}.

cited states are expected to be largely of $M1$ type. If the latter are pure $M1$ transitions, then the $B(M1)$ value for the transition to the $\frac{1}{2}-$ second excited state is 2.5 times larger than that for the transition to the $\frac{3}{2}-$ first excited state.

If the 1808.7-keV state consisted, as might be expected, of a fraction of the $p_{3/2}$ shell-model strength, coupled, probably, to other particle excitations, then a different pattern of deexcitation would evidently be observed, namely, strong $M1$ transitions to the $p_{3/2}$ and $p_{1/2}$ first and second excited states, respectively, and no $E2$ transition to the $f_{7/2}$ ground state. Conversely, the presence of the strong $E2$ ground-state transition, together with the fact that the energy of the 1808.7-keV state is comparable to that of the 1596-keV first excited 2+ state in Ce^{140} suggest that this state is a member of the core excitation multiplet arising from the coupling of an $f_{7/2}$ neutron to the 2+ state of the Ce^{140} core. The $\frac{5}{2}-'$ state at 1736 keV may be an additional member of this multiplet.

In a test of the hypothesis that the $\frac{3}{2}'$ state in Ce^{141} may be a core excitation state, we have carried out a calculation of the properties of the low-lying excited states in this nucleus based on the weak-coupling model.[26,27] Earlier work, for example, the calculation by Silverberg[28] on Tl^{205}, has demonstrated that this model may be as successful, in favorable cases, in predicting nuclear properties as more complicated shell-model calculations. The measured branching ratios of the transitions from the $\frac{3}{2}-'$ state should provide a sensitive test of this model. A further, less precise, test is also provided by the branching ratio of the transitions from the $\frac{5}{2}-$ state at 1497 keV.

B. Description of the Analysis

We assume that the single neutron outside the $N=82$ closed shell is weakly coupled to the surface of the $_{58}Ce^{140}$ core. The total Hamiltonian[26] may then be written as

$$H_T=H_n+H_s+H_{\rm int}, \quad (1)$$

where H_n represents the shell-model Hamiltonian for the single neutron, H_s describes the motion of the surface of the core (we consider only quadrupole deformation), and the interaction term

$$H_{\rm int}=-k(r)\sum_\mu \alpha_{2\mu}Y_{2\mu}(\Theta,\Psi)$$

defines the coupling between the particle, with coordinates (r, Θ, Ψ), and the core described by the parameter α.

We denote our basis states, the eigenfunctions of the uncoupled Hamiltonian, by

$$|lj, NR; IM\rangle, \quad (2)$$

where l and j refer to the single neutron, N is the number of phonons coupled to angular momentum R, and I is the total angular momentum with projection M.

The eigenstates of the total Hamiltonian are expressed in terms of the basis states (2) as

$$|IM\rangle=\sum_{lj,NR} c(lj, NR; IM)\,|lj, NR; IM\rangle. \quad (3)$$

The coefficients $c(lj, NR; IM)$ and the eigenvalues E were determined by diagonalizing the matrix $\langle I_fM_f\,|\,H_T\,|\,I_iM_i\rangle$.

In the present calculation, we only consider the basis states which arise from the coupling of the $f_{7/2}$, $p_{3/2}$, $p_{1/2}$, and $f_{5/2}$ neutron states with zero- or one-phonon states to total spins $\frac{7}{2}$, $\frac{3}{2}$, $\frac{1}{2}$, and $\frac{5}{2}$.

In this case, the only relevant nondiagonal matrix elements are[26]

$$\langle l_fj_f, 0\,0; I=j_f, M\,|\,H_{\rm int}\,|\,l_ij_i, 12; IM\rangle = -k(\hbar\omega/2C)^{1/2}(l_fj_f\,||\,Y_2\,||\,l_ij_i), \quad (4)$$

where k is the matrix element of $k(r)$ which we consider as a constant, $\hbar\omega$ is the phonon energy, C is the restoring force constant associated with the vibrations of the core, and the last factor is the reduced matrix element for the second-order harmonic, values of which have been tabulated in Ref. 26.

[26] A. Bohr and B. Mottelson, Kgl. Danske Videnskab. Selskab, Mat.-Fys. Medd. **27**, No. 16 (1953); K. W. Ford and C. Levinson, Phys. Rev. **100**, 1 (1955).
[27] B. J. Raz, Phys. Rev. **114**, 1116 (1959).
[28] L. Silverberg, Arkiv Fysik **20**, 355 (1961).

C. Transition Probabilities

The electric quadrupole and magnetic dipole reduced transition probabilities $B(E2)$ and $B(M1)$ may be expressed in terms of the reduced matrix elements $(I_f \| \mathcal{O}_\lambda \| I_i)$ as

$$B(\mathcal{O}_\lambda) = |(I_f \| \mathcal{O}_\lambda \| I_i)|^2/(2I_i+1),$$

where $\mathcal{O}_\lambda$ denotes the $E2$ or $M1$ operator.

The contribution of the core is separated from the contribution of the outside neutron, hence, we may write

$$(I_f \| \mathcal{O}_\lambda \| I_i) = (I_f \| \mathcal{O}_\lambda^{\text{core}} \| I_i) + (I_f \| \mathcal{O}_\lambda^{n} \| I_i).$$

Either term will have contributions from the different terms in (3). Thus,

$$(I_f \| \mathcal{O}_\lambda^{\text{core}(n)} \| I_i) = \sum_{l_f j_f N_f R_f, l_i j_i N_i R_i} c(l_f j_f N_f R_f; I_f)\, c(l_i j_i N_i R_i; I_i)\, (l_f j_f N_f R_f; I_f \| \mathcal{O}_\lambda^{\text{core}(n)} \| l_i j_i N_i R_i; I_i),$$

where[29]

$$(l_f j_f N_f R_f; I_f \| \mathcal{O}_\lambda^{\text{core}} \| l_i j_i N_i R_i; I_i) = (-1)^{j_f+R_i+I_f+\lambda} [(2I_f+1)(2I_i+1)]^{1/2} \begin{Bmatrix} R_f & I_f & j_f \\ I_i & R_i & \lambda \end{Bmatrix} (N_f R_f \| \mathcal{O}_\lambda^{\text{core}} \| N_i R_i) \delta_{j_f, j_i}$$

and

$$(l_f j_f N_f R_f; I_f \| \mathcal{O}_\lambda^{n} \| l_i j_i N_i R_i; I_i) = (-1)^{j_f+R_f+I_i+\lambda} [(2I_f+1)(2I_i+1)]^{1/2} \begin{Bmatrix} j_f & I_f & R_f \\ I_i & j_i & \lambda \end{Bmatrix} (l_f j_f \| \mathcal{O}_\lambda^{n} \| l_i j_i) \delta_{N_f, N_i} \delta_{R_f, R_i}.$$

The reduced $M1$ and $E2$ matrix elements, which appear on the right-hand side of the above expression, are as follows:

(a) $(NR \| M1^{\text{core}} \| NR) = (3/4\pi)^{1/2} (\mu_N/e) g_R [R(R+1)(2R+1)]^{1/2}$,

where μ_N is the nuclear magneton.

(b) $(N_f R_f \| E2^{\text{core}} \| N_i R_i) = (3/4\pi) Z R_0^2 (\hbar\omega/2C)^{1/2} (N_f R_f \| b \| N_i R_i)$,

where $R_0 = (1.2\times 10^{-13}) A^{1/3}$ cm and the values of the quantity $(N_f R_f \| b \| N_i R_i)$ have been tabulated by Raz[27] [the only nonzero matrix element $(N_f R_f \| b \| N_i R_i)$ which enters our calculation is that with $\Delta N = 1$; $\Delta R = 2$ and its value is $\sqrt{5}$].

(c) $$(l_f j_f \| M1^n \| l_i j_i) = \left(\frac{3}{4\pi}\right)^{1/2} \frac{\mu_N}{e} \mu_n \left(\frac{2(2j_i+1)(2j_f+1)}{(2l_i+1)}\right)^{1/2} (-1)^{j_i+l_i+3/2} \delta_{l_i, l_f}$$
$$\times \left\{ \delta_{j_i, j_f} \left(1 + \delta_{j, l+1/2} \left[\frac{l+\frac{3}{2}}{2(l+1)} \right]^{1/2} + \delta_{j, l-1/2} \left[\frac{l-\frac{1}{2}}{2l} \right]^{1/2} \right) - 1 \right\},$$

where the magnetic moment of the neutron is $\mu_n = 1.913$.

(d) $(l_f j_f \| E2^n \| l_i j_i) = 0$.

D. Parameters

The main purpose of this calculation was to investigate whether we can explain the measured branching ratios of the transitions from the 1808.7- and 1497.3-keV states in terms of the weak-coupling model. We have endeavored to keep the calculation as simple as possible by excluding states involving two or more phonons. As a result, we expect the model to reproduce the spectrum only approximately. For this reason, a search for the best over-all fit adjusting parameters was avoided and we have sought to fix all of them *a priori*. The several parameters involved in the calculation are associated with different terms of the total Hamiltonian (1). Those associated with the surface Hamiltonian H_s were fixed by making use of the data currently available on Ce^{140}. Thus, the energy (1.596 MeV) of the first excited 2^+ state of Ce^{140} was assumed to be the phonon energy $\hbar\omega$. The restoring force constant[30] $C = 366$ MeV or the more familiar quantity $\hbar\omega/2C = 2\times 10^{-3}$ was extracted from the value[31] $B(E2, 0+ \rightarrow 2+) = (3.15\times 10^{-49}) e^2$ cm^4 for Ce^{140}. The choice of the gyromagnetic factor g_R of the core is of particular importance for the evaluation of the $M1$ matrix elements of the 1146.6-keV transition (see Sec. V C). Because of the short lifetime of the 2+ state in Ce^{140} an experimental value for this quantity is not available. We have used the value $g_R = 0.95$ calculated by Kisslinger and Sorensen.[32] This relatively

[29] A. de-Shalit and I. Talmi, *Nuclear Shell Theory* (Academic Press Inc., New York, 1963).

[30] C. Y. Wong, Nucl. Data **A4**, 271 (1968).

[31] P. H. Stelson and L. Grodzins, Nucl. Data **A1**, 21 (1965).

[32] L. Kisslinger and R. Sorensen, Rev. Mod. Phys. **35**, 853 (1963).

TABLE IV. Eigenvalues and wave functions of the $\frac{7}{2}$-, $\frac{3}{2}$-, $\frac{1}{2}$-, and $\frac{5}{2}$-states in Ce^{141}.

States I, π	Eigenvalues E_I (MeV)	Basis states $\|lj, NR\rangle$ and coefficients $c(lj, NR, I)$				
		$f_{7/2},00$	$f_{7/2},12$	$p_{3/2},12$	$f_{5/2},12$	
$\frac{7}{2}-$	−0.281	0.943	−0.278	0.176	−0.051	
		$f_{7/2},12$	$p_{3/2},00$	$p_{3/2},12$	$p_{1/2},12$	$f_{5/2},12$
$\frac{3}{2}-$	0.403	0.546	0.801	−0.170	−0.151	0.092
$\frac{3}{2}-'$	2.036	0.814	−0.440	0.294	0.211	−0.116
		$p_{3/2},12$	$p_{1/2},00$	$f_{5/2},12$		
$\frac{1}{2}-$	0.904	0.335	0.884	0.325		
		$f_{7/2},12$	$p_{3/2},12$	$p_{1/2},12$	$f_{5/2},00$	$f_{5/2},12$
$\frac{5}{2}-$	1.235	0.493	−0.140	0.219	0.803	−0.211
$\frac{5}{2}-'$	1.706	0.869	0.108	−0.158	−0.433	0.148

high value for g_R reflects the predominant influence of the looser proton core ($Z=58$) over the neutron core ($N=82$).[33] Although the success of such calculations is erratic, they have been most successful in the region just above $Z=50$.[34]

The strength of the interaction was fixed by an arbitrary choice of the value $k=40$ MeV given in Ref. 26. A more convenient and customary measure of the coupling strength is given by the dimensionless quantity $x=k(5/16\pi\hbar\omega C)^{1/2}$. The smallness of x provides a measure of the validity of the weak-coupling calculation. The choice of $k=40$ MeV corresponds to a value of $x=0.5$, which lies within the range of validity of the calculation and is similar to the values of x used in previous such calculations.[26,28]

Finally, we need to specify the single-particle energies $\epsilon_{f7/2}$, $\epsilon_{p3/2}$, $\epsilon_{p1/2}$, and $\epsilon_{f5/2}$. Since data on these quantities are not available, they were chosen so that the calculation would reproduce the experimental energies of the first $\frac{3}{2}-$, $\frac{1}{2}-$, and $\frac{5}{2}-$ excited states with $\epsilon_{f7/2}$ set equal to zero. The energies of the $\frac{5}{2}-'$ and $\frac{3}{2}-'$ states and the branching ratios of the transitions from the $\frac{3}{2}-'$ and $\frac{5}{2}-$ states were calculated with the above choice of parameters.

Table III summarizes the values of the parameters used in the present calculations.

E. Results of the Calculation

Table IV shows the eigenvalues and eigenvectors obtained for the states in which we are interested. The $\frac{5}{2}-'$ and $\frac{3}{2}-'$ states are predominantly ($\sim$70%) due to an $f_{7/2}$ neutron coupled to the one-phonon state. The calculated level energies for these states, 1.99 and 2.32 MeV, respectively, are larger than the experimental values by about 0.5 MeV. Although we have not attempted to adjust the parameters involved in the calculation to obtain an optimum fit, a simple estimate indicates that a reduction of the interaction strength by a factor of 2 ($k=20$ MeV) would produce level energies in good agreement with experiment (after the single-particle energies have been readjusted). At the same time the agreement (see below) between the experimental and calculated branching ratios would be worse. A least-squares fitting procedure to adjust the parameter k would certainly improve the over-all agreement obtained with experiment but would not alter our conclusions significantly. Therefore, it was not attempted.

At the same time, one must bear in mind that the inclusion of states involving two phonons would tend to lower the energies of both the $\frac{3}{2}-'$ and $\frac{5}{2}-'$ states without affecting the energies of the other states very much.

A more meaningful test of the model is obtained from the study of relative transition probabilities. Table V shows the calculated transition probabilities and a comparison of the computed branching ratios with those measured in the (n, γ) reaction. The first column lists the transitions of interest. Columns 2–4 give the calculated values of the reduced transition probability $B(E2)$, transition probability $T(E2)$, and the transition probability in single-particle units (Moszkowski's estimate with the statistical factor $S=1$). The corresponding quantities for the $M1$ transitions are given in the same order in columns 5–7. The calculated mixing ratio for each transition, with the exception of the pure $E2$ $\frac{3}{2}'\rightarrow\frac{7}{2}$ transition, is given in column 8. With this exception the transitions are almost pure $M1$. The calculated branching ratios are shown in column 9. These values are to be compared with the experimental branching ratios in the final column. The agreement is remarkably good. The $\frac{3}{2}'\rightarrow\frac{3}{2}$ $M1$ transition is found to be weak (0.1) in terms of single-particle units so that its intensity becomes comparable with the intensity of the other two transitions depopulating the $\frac{3}{2}'$ state. The hindrance of this transition originates in the particular configuration of the $\frac{3}{2}'$ and $\frac{3}{2}$ states. If we ignore all

[33] We are indebted to Dr. J. Weneser for bringing this point to our attention.

[34] L. Grodzins, Ann. Rev. Nucl. Sci. **18**, 291 (1968).

TABLE V. Calculated transition probabilities and branching ratios and experimental branching ratios in Ce^{141}. The notation $\frac{3}{2}'$ stands for second excited $\frac{3}{2}$ state. The single-particle transition probabilities $T_{sp}(\lambda)$ used to derive the ratios given in columns 4 and 7 are those of Moszkowski with the statistical factor S equal to 1.

Transition $I_i \to I_f$	$B(E2)/e^2$ cm^4	$T(E2)$ sec^{-1}	$\frac{T(E2)}{T_{sp}(E2)}$	$B(M1)/e$ cm^2	$T(M1)$ sec^{-1}	$\frac{T(M1)}{T_{sp}(M1)}$	$\delta^2=\frac{T(E2)}{T(M1)}$	Branching ratios Calc	Expt
$\frac{3}{2}' \to \frac{7}{2}$	2.47×10^{-50}	5.9×10^{12}	2.6	...	...	...	∞	1	1
$\frac{3}{2}' \to \frac{3}{2}$	0.58	0.15	0.63	1.7×10^{-29}	4×10^{12}	0.1	0.04	0.68	1.7 ± 0.8
$\frac{3}{2}' \to \frac{1}{2}$	0.47	0.009	0.56	6.3	3	0.35	0.003	0.51	0.8 ± 0.4
$\frac{5}{2} \to \frac{7}{2}$	1.20	1.1	1.23	9.6	51	0.54	0.02	1	1
$\frac{5}{2} \to \frac{3}{2}$	0.24	0.013	0.26	1.0	1	0.06	0.013	0.02	0.14 ± 0.10

but the two predominant terms of the wave function, we find (Table IV)

$$|\tfrac{3}{2}'\rangle = 0.814\,|f_{7/2}12;\tfrac{3}{2}\rangle - 0.440\,|p_{3/2}00,\tfrac{3}{2}\rangle$$

and

$$|\tfrac{3}{2}\rangle = 0.546\,|f_{7/2}12;\tfrac{3}{2}\rangle \quad 0.801\,|p_{3/2}00,\tfrac{3}{2}\rangle$$

so that the $|f_{7/2}12;\frac{3}{2}\rangle \to |f_{7/2}12;\frac{3}{2}\rangle$ contribution to the $M1$ single-particle matrix element is almost cancelled by the $|p_{3/2}00;\frac{3}{2}\rangle \to |p_{3/2}00;\frac{3}{2}\rangle$ term. Thus, most of the strength of this transition (99%) comes from the matrix element of the $M1$ core operator. (In this case only the $|f_{7/2}12;\frac{3}{2}\rangle$ terms contribute, since $R=0$ for the $|p_{3/2}00,\frac{3}{2}\rangle$ terms.)

The $E2$ transition to the ground state is calculated to be 2.5 times slower than that of the pure core [$B(E2, 2^+ \to 0^+)$ for Ce^{140}] and 2.6 times the single-particle strength. The $\frac{3}{2}' \to \frac{1}{2}$ $M1$ transition is calculated to be largely (90%) of single-particle character with the two main terms,

$$|f_{7/2}12;\tfrac{3}{2}\rangle \to |f_{5/2}12;\tfrac{1}{2}\rangle \quad \text{and} \quad |p_{3/2}00;\tfrac{3}{2}\rangle \to |p_{1/2}00,\tfrac{1}{2}\rangle,$$

adding coherently.

The branching ratio from the $\frac{5}{2}-$ state has a large experimental error. The predicted value seems to be small compared with the measured value but they are in reasonable qualitative agreement.

It is also of interest to compare the measured spectroscopic factors[8,12] (S_{dp} and $S_{pp'}$) for the (d, p) and (p, p') reactions with the squares of the amplitudes $c^2(lj, 00, I)$ of the single-particle states. Table VI summarizes the relevant information. Columns 1 and 2 list the energies, spins, and parities of the levels and column 3 lists the calculated values of $c^2(lj, 00, I)$ for these levels. The corresponding values of $S_{pp'}$ and S_{dp} from Refs. 12 and 8 are given in columns 4 and 5. We find that there is a reasonable agreement between theory and experiment for the ground state and first excited state, but that the $\frac{1}{2}-$ and $\frac{5}{2}-$ states are not as pure as predicted. The calculated value $c^2(f_{5/2}00, S)=0.2$ for the $\frac{5}{2}-'$ state is in good agreement with the measured value of $S_{pp'}$ but disagrees with the value of S_{dp}.

We conclude by noting that the gross features of the low-lying excitations in Ce^{141} can be understood in terms of our relatively simple description based on the weak-coupling model.[26,27] Because of the simplifications made in the course of the calculation, namely, the exclusion of states involving two or more phonons and of the $h_{9/2}$ and $i_{13/2}$ shell-model orbits, and the fixing of all parameters *a priori*, the calculation is not expected to describe all the properties of this nucleus in detail. We find that the calculated branching ratios of transitions from the $\frac{3}{2}-'$ and $\frac{5}{2}-$ states are in good agreement with experiment. Only moderate agreement is found with the experimental values of S_{dp} and $S_{pp'}$, and the predicted energies of the $\frac{5}{2}-'$ and $\frac{3}{2}-'$ states are too high by $\approx$0.5 MeV.

TABLE VI. Comparison of spectroscopic factors obtained in the $Ce^{140}(p, p')$ and $Ce^{140}(d, p)$ reactions with squares of the coefficients $c(lj, 00, I)$.

Level energy (MeV)	I, π	$c^2(lj, 00, I)$ [a]	$S_{pp'}$ [b]	S_{dp} [c]
0	$\frac{7}{2}-$	0.89	0.78	0.89
0.662	$\frac{3}{2}-$	0.64	0.42	0.42
1.137	$\frac{1}{2}-$	0.78	0.32	0.38
1.497	$\frac{5}{2}-$	0.64	0.31	0.30
1.736	$\frac{5}{2}-$	0.19	0.25	0.38
1.808	$\frac{3}{2}-$	0.19	...	...

[a] From Table III.
[b] Reference 12.
[c] Reference 8.

VI. COMPARISON WITH OTHER EVEN-Z, $N=83$ NUCLEI

It is of considerable interest to compare the level scheme of Ce^{141} with the level schemes of the other even-Z, $N=83$ nuclei. Figure 5 shows the known energy levels below 3.5 MeV in $_{54}Xe^{137}$, $_{56}Ba^{139}$, $_{58}Ce^{141}$, $_{60}Nd^{143}$, and $_{62}Sm^{145}$. Where the spin and parity of a level are known they are shown on the left-hand side of the level. The measured strength of excitation of the level

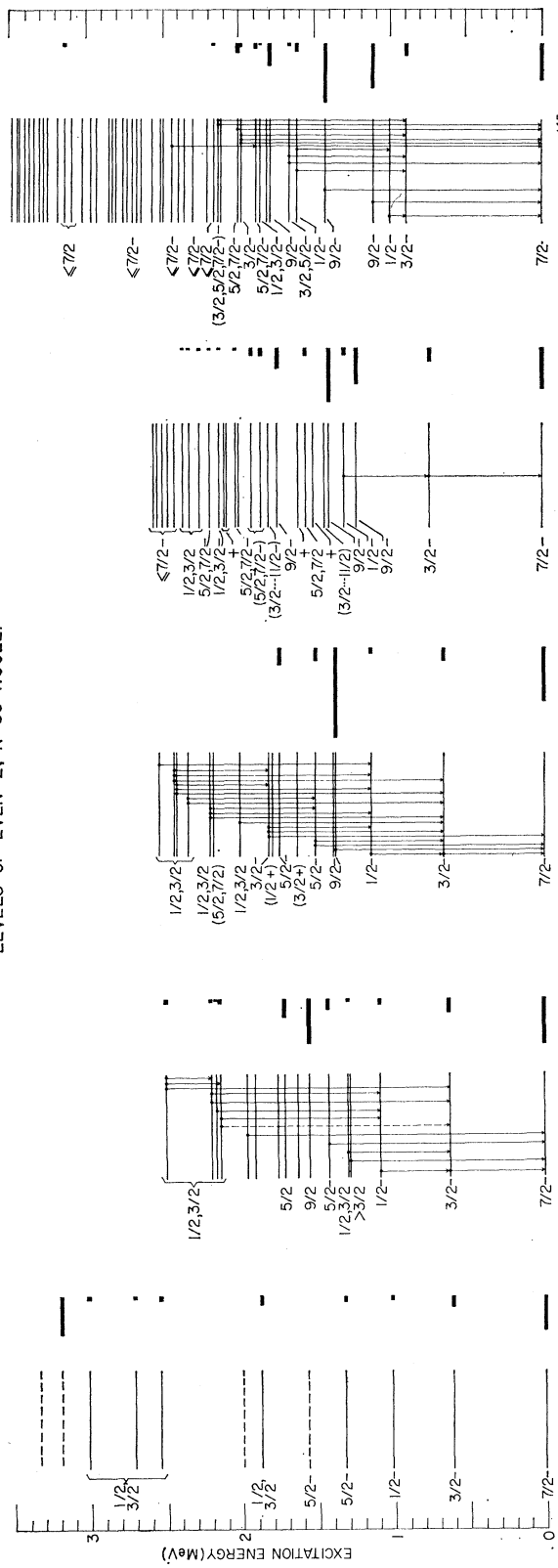

FIG. 5. This figure summarizes the information which is currently available on energy levels below 3.5 MeV in the nuclei Xe^{137}, Ba^{139}, Ce^{141}, Nd^{143}, and Sm^{145}, which contain 83 neutrons and an even number of protons. The excitation energy (in MeV) above the ground state is indicated by the vertical scale on both sides of the figure. Where the spin and parity of a level are known they are shown on the left-hand side of the level. The measured strength of excitation of the level in the (d, p) reaction $G_{dp}=(2J+1)\,S$, where S is the spectroscopic factor, is indicated by the length of the block on the right-hand side of those levels for which it has been measured. Where γ-ray or conversion electron studies have been undertaken the assigned transitions are indicated by vertical arrows joining the two levels between which the transition takes place. Our current knowledge of these nuclei is derived mainly from studies of the (d, p), (p, p'), and (n, γ) reactions and of radioactive decay schemes (see text). The Ba^{139} level scheme is that given in Ref. 24. The level scheme for Ce^{141} is essentially that obtained in the present paper (see Fig. 4). The Xe^{137}, Nd^{143}, and Sm^{145} level schemes are based on Refs. 35–43.

in the (d, p) reaction $G_{dp}=(2J+1)S$, where S is the spectroscopic factor, is indicated by the length of the block on the right-hand side of the level.

The information used to prepare Fig. 5 comes from a wide variety of sources. Because of the closed-shell nature of the target and the resulting simplicity of the states in the product nuclei the (d, p) reaction is perhaps the most convenient and widely used method of studying these nuclei. Measurements of the angular distributions of the outgoing protons provide information on the spins and parities of many of the levels, and spectroscopic factors, where measured, give a measure of the strength of the predominant single-particle configuration in the level.

The study of isobaric analog resonances in the scattering of protons from $N=82$ target nuclei also provides information on the analogs of levels in the $N=83$ nuclei. The spins and parities of the four or five lowest-lying levels in each of these nuclei have been measured in studies of such reactions. Spectroscopic factors have also been measured for some levels in these (p, p') reaction studies, and it has been shown[12] that they are in good agreement with spectroscopic factors measured in the (d, p) reaction.

The information available on the electromagnetic decay of levels in these nuclei is essentially restricted to Ba^{139}, Ce^{141}, and Sm^{145}. In the first two cases, the information comes from the $Ba^{138}(n, \gamma)Ba^{139}$ (see Ref. 24) and $Ce^{140}(n, \gamma)Ce^{141}$ (see Fig. 4) reactions. The γ decay of levels in Sm^{145} has been studied by Christensen, Herskind, Borchers, and Westgaard[35] in the $Sm^{144}(d, p\gamma)Sm^{145}$ reaction, and by Antonevna, Bashilov, Dzhelepov, Kaun, Mayer, and Smirnov[36] and Alexandrov and Nikitin[37] in the decay of Eu^{145}.

The amount of information available on these five nuclei varies considerably from one nucleus to another. Xe^{137} is the least studied because of the experimental difficulties of producing a suitable gaseous target with separated Xe^{136} for charged particle reaction studies. Nevertheless, the $Xe^{136}(d, p)Xe^{137}$ and $Xe^{136}(p, p')Xe^{136}$ reactions have been studied by Schneid and Rosner[38] and by Moore, Riley, Jones, Mancusi, and Foster,[39] respectively. The spins and parities shown in Fig. 5 for the ground state and first four excited states were deduced by Moore *et al.*[39]

The level scheme shown for Ba^{139} is that given in Ref. 24.

The level scheme for Ce^{141} is that obtained in the present work (see Fig. 4) with the addition of the positive-parity levels at 1620 and 1780 keV which were observed by Fulmer, McCarthy, and Cohen[7] in the $Ce^{142}(d, t)$ reaction.

The Nd^{143} level scheme is mainly based on the $Nd^{142}(d, p\gamma)Nd^{143}$ and $Nd^{143}(d, d')Nd^{143}$ reaction studies of Christensen *et al.*,[35] Zaidi *et al.*[10] Wurm, von Brentano, Grosse, Seitz, Wiedner, and Zaidi,[40] and Harney *et al.*[12] have studied the $Nd^{142}(p, p')Nd^{142}$ reaction and they obtain spectroscopic factors, spins, and parities for several of the low-lying levels in agreement with those measured by Christensen *et al.*[35]

Several authors[35,41–43] have studied the $Sm^{144}(d, p)Sm^{145}$ reaction and their results are in good agreement. Moore and Jolly[43] and Wurm *et al.*[40] have studied the $Sm^{144}(p, p')Sm^{144}$ reaction and the spins and parities they assign are in good agreement with those obtained in the (d, p) reaction studies. Christensen *et al.*[35] studied the $Sm^{144}(d, p\gamma)Sm^{145}$ reaction and the γ rays observed by them are in good agreement with those observed by Antonevna *et al.*[36] and by Alexandrov and Nikitin.[37] The first two of these groups agree about the placement of the observed γ rays, but disagree with Alexandrov *et al.* about the decay of the level at 1660 keV and the existence of a level at 1140 keV. The results of Refs. 35 and 36 were preferred here with the 1660-keV level decaying to levels at 0, 894, and 1004 keV. The possible level at 1140 keV was not included in the figure. The level at 1610 keV has been assigned spin and parity $\frac{1}{2}-$ by Christensen *et al.*[35] and $\frac{3}{2}-$ by Jolly and Moore.[42] The measured spectroscopic factor ($S=0.4$) and the level energy are consistent with the systematic behavior of the $p_{1/2}$ state. The only other candidate for this rôle is the $\frac{1}{2}-$ state at 1004 keV which is not excited directly in the (d, p) reaction and whose energy does not fit the trend established for the $p_{1/2}$ state in the lower-Z nuclei. The available evidence suggests that the level at 1610 keV is a $\frac{1}{2}-$ state and that it contains a large part of the $p_{1/2}$ strength. It has been labelled $\frac{1}{2}-$ here.

The level structure of these even-Z $N=83$ nuclei is expected to be particularly simple with the lowest-lying levels corresponding to a single neutron in the $2f_{7/2}$, $3p_{3/2}$, $3p_{1/2}$, $2f_{5/2}$, $1h_{9/2}$, and $1i_{13/2}$ orbits. The mixing of single-particle states with states formed by the coupling of the single-particle states with the collective states of the core is expected to produce a large number of states with a wide variety of spins at slightly higher energies. The single-particle strength

[35] P. R. Christensen, B. Herskind, R. R. Brochers, and L. Westgaard, Nucl. Phys. **A102,** 481 (1967).
[36] N. M. Antonevna, A. A. Bashilov, B. S. Dzhelepov, K. G. Kaun, A. F. A. Meyer, and V. B. Smirnov, Zh. Eksperim. i Teor. Fiz. **40,** 23 (1961) [English transl.: Soviet Phys.—JETP **13,** 15 (1961)].
[37] Yu. A. Alexandrov and M. K. Nikitin, Bull. Acad. Sci. USSR, Ser. Phys. **25,** 1181 (1960).
[38] E. J. Schneid and B. Rosner, Phys. Rev. **148,** 1241 (1966).
[39] P. A. Moore, P. J. Riley, C. M. Jones, M. D. Mancusi, and J. L. Foster, Jr., Phys. Rev. Letters **22,** 356 (1969).
[40] J. P. Wurm, P. von Brentano, E. Grosse, H. Seitz, C. A. Wiedner, and S. A. A. Zaidi, in *Isobaric Spin in Nuclear Physics,* edited by J. D. Fox and D. Robson (Academic Press Inc., New York, 1966), p. 790.
[41] R. A. Kenefich and R. K. Sheline, Phys. Rev. **139,** B1479 (1965).
[42] R. K. Jolly and C. F. Moore, Phys. Rev. **145,** 918 (1966).
[43] C. F. Moore and R. K. Jolly, Phys. Letters **19,** 138 (1965).

is thus expected to be distributed over several states. That these expectations are largely borne out by experiment is evident from a study of Fig. 5.

The ground state clearly exhausts a large fraction of the $2f_{7/2}$ strength in all cases with values of S ranging from 0.58 in Xe^{137} and Sm^{145} to a maximum of 0.89 in Ca^{141}. The first excited state, which increases steadily in energy with increasing Z, is predominantly due to a $3p_{3/2}$ neutron and is roughly constant in strength as a function of Z. The $3p_{1/2}$ state exhibits very similar behavior. For both of these states $S\approx 0.4$ in all five nuclei. The remainder of the single-particle strength is distributed among higher-lying levels. The $2f_{5/2}$ state is more fragmented although one or two levels take a moderately large fraction of the strength in every case. This state appears to become more fragmented with increasing Z. No information is available on the $h_{9/2}$ state in Xe^{137}. As we proceed from Ba^{139} to Sm^{145}, this state clearly becomes more fragmented. In Ba^{139}, the $\frac{9}{2}-$ state at 1550 keV has $S=0.6$. In Ce^{141} the doublet at 1374–1383 keV has $S\approx 1.2$. In Nd^{143} the strength is spread over the states at 1226, 1405, and 1740 keV ($\sum S=1.46$). In Sm^{145} three $\frac{9}{2}-$ states are known with $\sum S=0.6$. The missing strength for this state in Sm^{145} must be distributed among several levels.

Above 1.5 MeV, the level density increases very rapidly and it becomes difficult to make any positive statement about the character of the observed levels. This behavior is consistent with the expected onset of levels due to the coupling of a single particle to the excited states of the core, and other more complicated configurations.

Some individual states are of particular interest. The $\frac{1}{2}-$ state at 1004 keV in Sm^{145}, the doublet at $\sim$1290 keV in Ba^{139}, and the 1660-keV level in Sm^{145} have small spectroscopic factors. This may indicate that they are due to single-particle states coupled to the 2+ excited state of the semimagic core. If the spin of the 1660-keV level in Sm^{145} is $\frac{3}{2}-$ the observed branching ratio, with an $E2$ transition to the ground state competing favorably with $M1$ transitions to the first and second excited states, would support such an interpretation, as in the similar case of the 1808.7-keV level in Ce^{141}, which is discussed in Sec. V. In this context, it should be noted that it was not possible in the $Ba^{138}(n, \gamma)Ba^{139}$ reaction study of Ref. 24 to observe a transition to the ground state from the state at 1292.6 keV because of the presence of a masking transition in the background. The observation of such a transition would be of importance for the interpretation of the character of this state, since its presence might indicate that this state involves the coupling of a single-particle state to an excited state of the core.

Very little information is available on even-parity states in these nuclei. Fulmer, McCarthy, and Cohen[7] have observed states at 1620 and 1780 keV in the $Ce^{142}(d, t)Ce^{141}$ reaction which they interpret as the $d_{3/2}$ and $s_{1/2}$ hole states. A few even-parity states have also been identified by Christensen *et al.*[35] in the $Nd^{143}(d, d')Nd^{143}$ reaction. Clearly, we require a great deal more information on such levels.

Figure 5 clearly points to several other gaps in our knowledge of these nuclei. As yet we know nothing about the γ decay of the levels in Xe^{137} and Nd^{143}. The decay of levels in both these nuclei may be studied with the (n, γ) reaction although it is difficult to obtain a suitable target of separated Xe^{136}. Many spins and parities are as yet unmeasured in all five nuclei and spectroscopic factors have been measured for only a small number of states, particularly in Xe^{137} and Ce^{141}.

In summary, we may say that, as expected, in these $N=83$ nuclei we do see evidence of single neutron particle states and of single-particle states coupled to the excited states of the core, but as yet the experimental information available is too limited to provide a more detailed description of their properties.

ACKNOWLEDGMENTS

We should like to acknowledge the advice and encouragement of G. Scharff-Goldhaber and A. W. Sunyar. We should also like to thank J. Weneser for an interesting and stimulating discussion of the structure of Ce^{141}. Our thanks are also due to E. der Mateosian for his criticism of this paper.